Supplemental information

Multifaceted N-degron recognition and ubiquitylation by GID/CTLH E3 ligases

Jakub Chrustowicz*, Dawafuti Sherpa*, Joan Teyra, Mun Siong Loke, Grzegorz M. Popowicz, Jerome Basquin, Michael Sattler, J. Rajan Prabu, Sachdev S. Sidhu, Brenda A. Schulman#

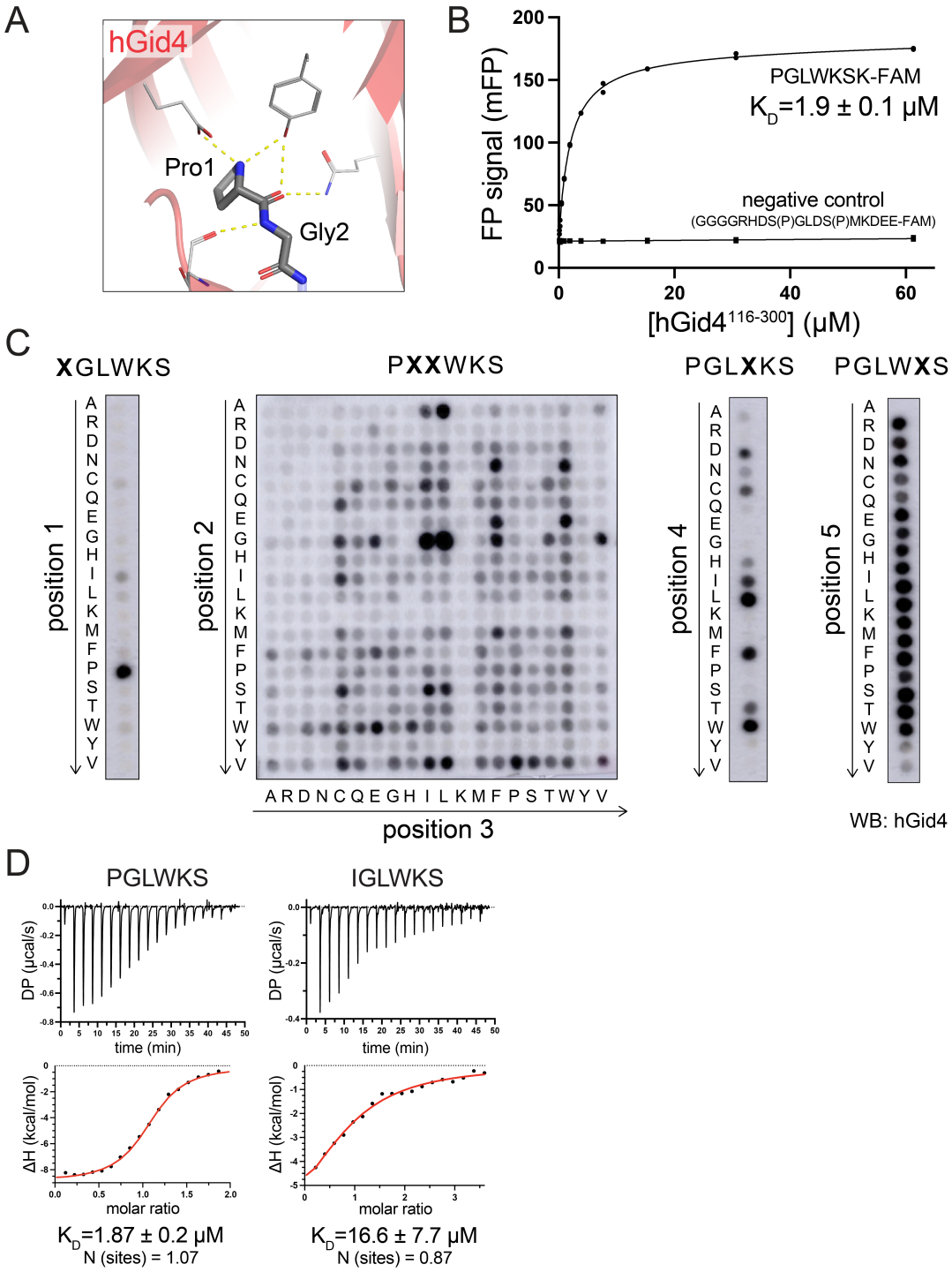

Figure S1: Characterization of hGid4 specificity toward a Pro/N-terminal peptide

A. Close-up of hGid4 interactions with first two residues of the PGLW peptide (PDB ID: 6CDC)
B. Fluorescence polarization (FP) experiment to quantify binding of fluorescent PGLWKS (C-terminally labelled with fluorescein) to hGid4 (Δ1-115). Fitting the FP values at increasing hGid4 concentrations to one site binding model yielded a dissociation constant (K_D). A non-hGid4 binding fluorescent peptide has been included as a negative control.
C. Peptide spot arrays to systematically screen the influence of amino acid substitutions at various positions of the PGLWKS sequence on hGid4 (Δ1-99) binding. Binding of hGid4 to generated peptide derivatives was visualized by immunoblotting with anti-hGid4 antibodies and chemiluminescence.
D. Control ITC measurement to quantify binding of the previously identified sequences to hGid4 (Δ1-115)

A

This study

peptide	K_D (μM)
FDVSWFMG	0.6
VDVNSLWA	1.3
WDVSWV	7.1
PDVSWFMG	0.6

Dong et al. 2018

peptide	K_D (μM)
PGLWKS	1.9
PGLW	2.5
PGLYKS	3.1
PGLHKS	3.6
PGLSKS	5.6
PALWKS	9.3
PGMWKS	13.5
PGLGKS	17.7
PSRV	19.4
PGLEKS	24.9
PGSWKS	33.8
PGYWKS	34.5
PHRV	35.2
PGQWKS	62.1

Dong et al. 2020

peptide	K_D (μM)
IGLWKS	16
LGLWKS	21
VGLWKS	36
FGLWKS	40
MGLWKS	72

B

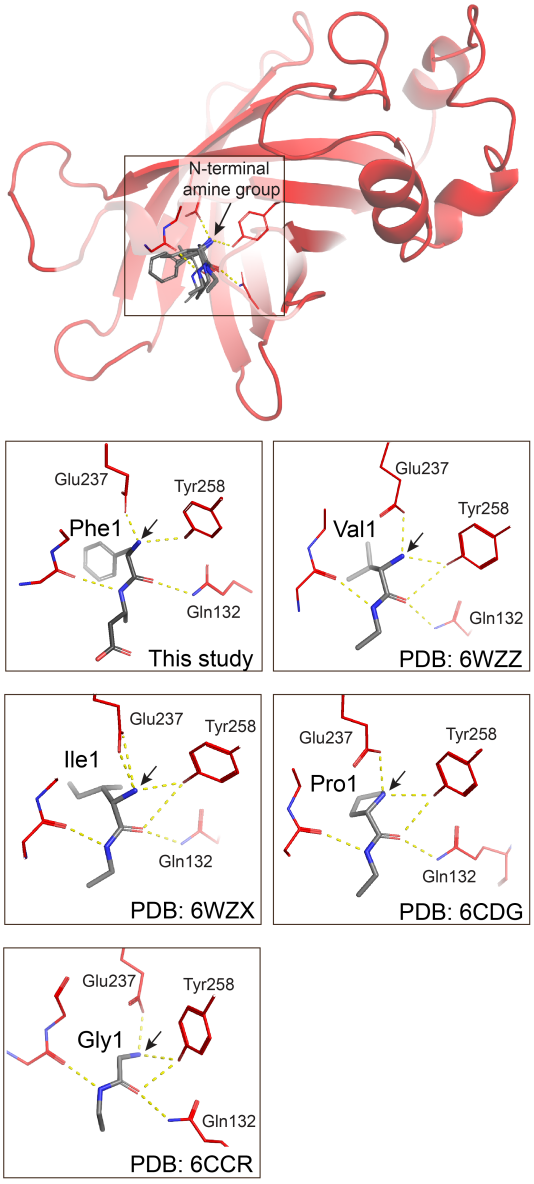

Figure S2: Recognition of diverse peptide sequences by hGid4

A. Table summarizing dissociation constants (K_D) of various peptides binding to hGid4 measured with ITC in this and the previous studies.

B. Overlay of FDVSWFMG-bound hGid4 with the published coordinates of hGid4 (top, first two residues of interacting peptides in all structures shown as grey sticks). The common binding mode of first two N-terminal peptide residues is shown for each structure separately (bottom). Black arrows indicate positions of N-terminal amine groups.

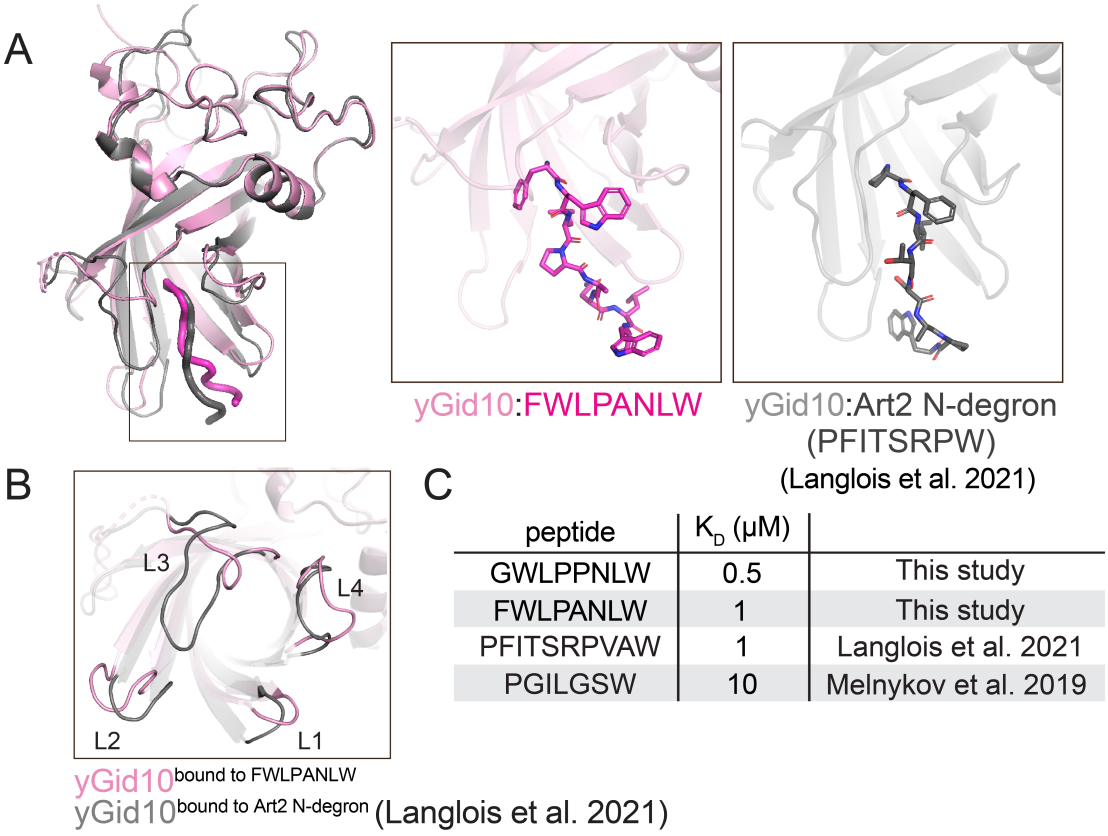

peptide	K_D (μM)	
GWLPPNLW	0.5	This study
FWLPANLW	1	This study
PFITSRPVAW	1	Langlois et al. 2021
PGILGSW	10	Melnykov et al. 2019

Figure S3: Binding specificity of yGid10

A. Overlay of yGid10 (Δ1-64, Δ285-292) structures (left) bound to FWLPANLW peptide and Pro/N-degron of yGid10 substrate Art2 (Langlois et al. 2021) (shown as magenta and grey ribbons, respectively). Close-ups of both peptides binding to the same yGid10 substrate binding tunnel (middle and right).
B. Conformational flexibility of yGid10 substrate-binding loops revealed by superimposing of yGid10 structures bound to FWLPANLW (pink) and Art2 Pro/N-degron (Langlois et al. 2021, grey).
C. Table summarizing dissociation constants (K_D) of various peptides binding to yGid10 measured with ITC in this and the previous studies.

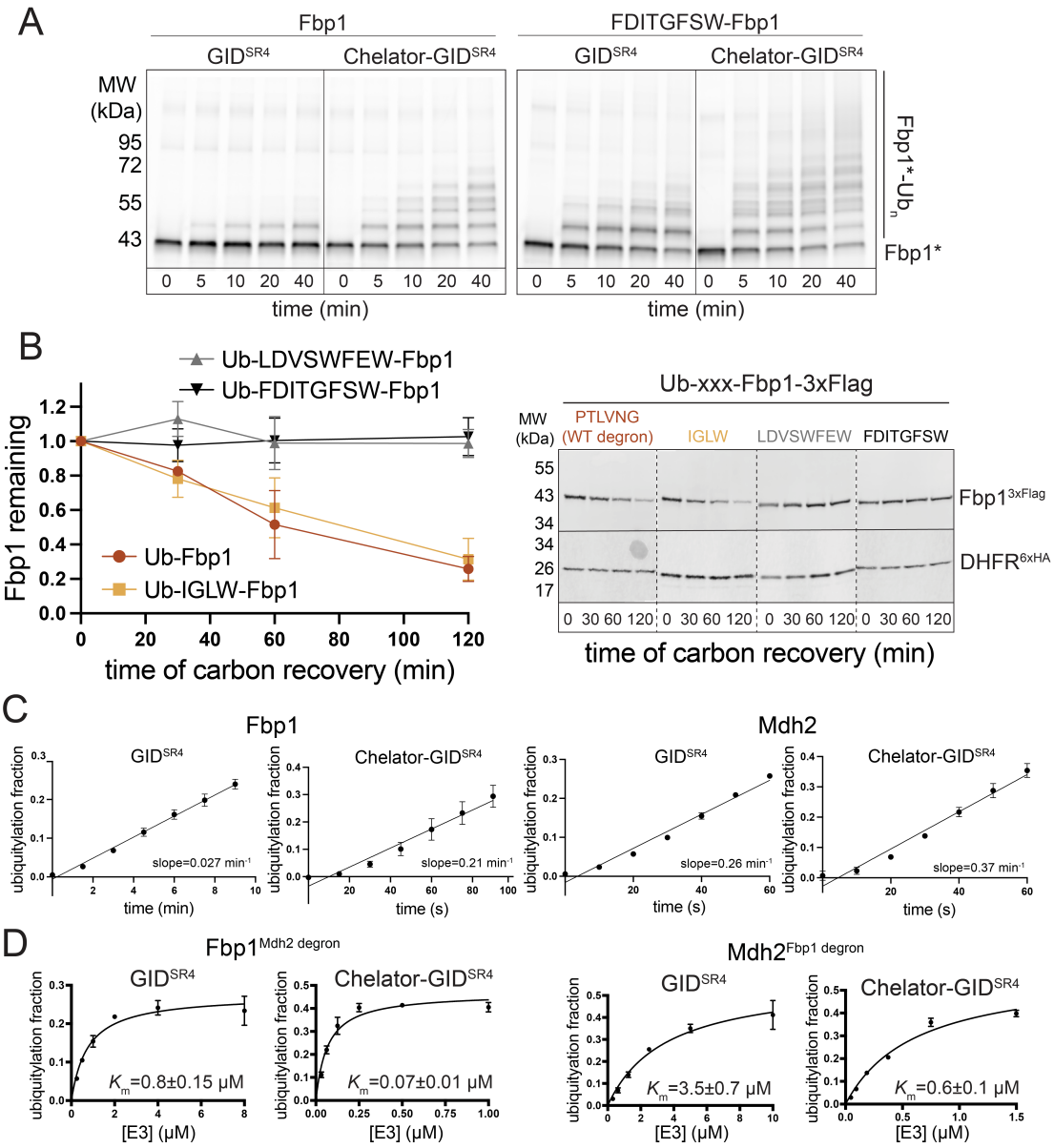

Figure S4: Effect of various N-terminal sequences on substrate targeting by GID

A. *In vitro* ubiquitylation assays probing the ability of the high-affinity FDITGFSW sequence to mediate ubiquitylation of the full-length substrate Fbp1 (tested by swapping its native degron with FDITGFSW) by two GID E3 ligase complex assemblies (GID^{SR4} and Chelator-GID^{SR4}). Both the WT and the degron-swapped Fbp1 were C-terminally labeled with fluorescein (indicated by an asterisk).

B. *In vivo* glucose-induced degradation of exogenously expressed and C-terminally 3xFlag-tagged Fbp1 derivatives whose N-termini were exchanged with the high-affinity binding sequences LDVSWFEW and FDITGFSW as well as a control IGLW sequence. To enable exposure of the hydrophobic N-termini, all Fbp1 versions were expressed as N-terminal fusions to ubiquitin, which is removed by cellular deubiquitylating enzymes. Levels of the substrates were quantified as in Fig. 6C based on immunoblots detecting Fbp1-3xFlag and DHFR-6xHA (right) and plotted as a function of time in glucose-rich conditions (left). Error bars in the plot represent standard deviation (n=3), whereas points represent the mean.

C. Time-courses of Fbp1 and Mdh2 ubiquitylation by GID^{SR4} and Chelator-GID^{SR4} employed to determine k_{cat} values (Fig. 5C).

D. Plots showing fraction of *in vitro*-ubiquitylated degron-swapped Fbp1 and Mdh2 as a function of varying concentrations of GID^{SR4} or Chelator-GID^{SR4}. Fitting to Michaelis-Menten equation yielded K_m values. Error bars represent standard deviation (n=2).

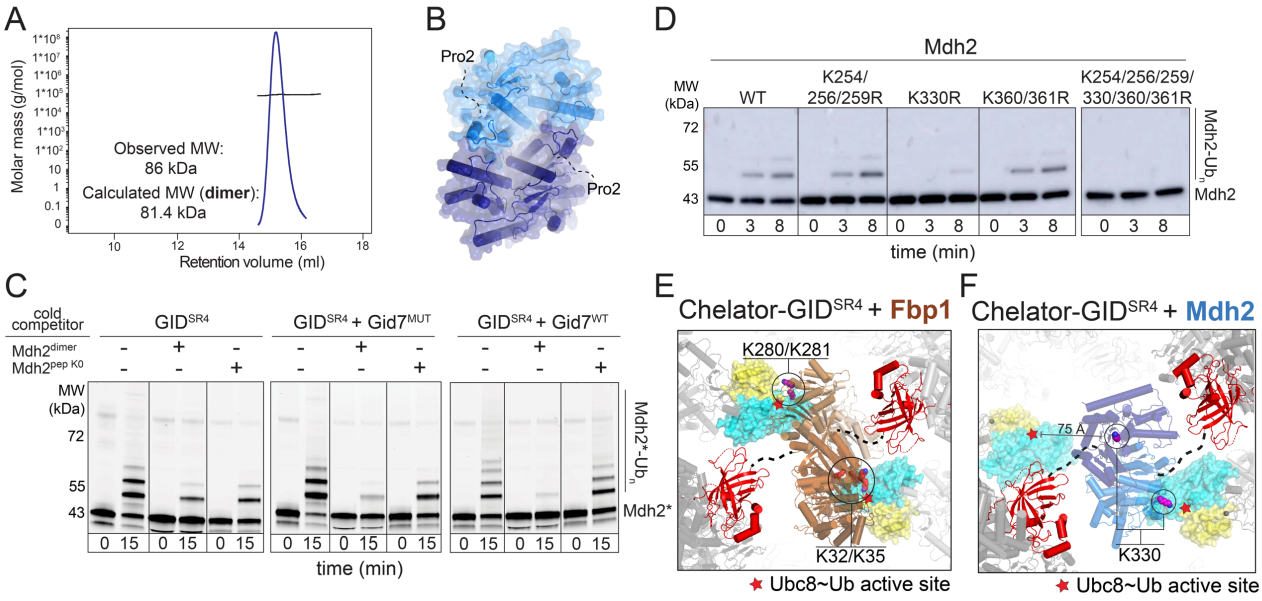

Figure S5: Differential targeting of Fbp1 and Mdh2 by Chelator-GID^{SR4}

A. SEC-MALS analysis of Mdh2 oligomeric state
B. Homology model of Mdh2 with unstructured Pro/N-degrons represented as dotted lines
C. Competitive ubiquitylation assays probing avid binding of Mdh2 to Chelator-GID^{SR4}. Ubiquitylation of fluorescent Mdh2 by monovalent (GID^{SR4} alone or mixed with Gid7$^{286-745}$ mutant) or divalent (Chelator-GID^{SR4}) version of GID E3 was competed with monodentate (Mdh2$^{pep\ K0}$ - lysineless peptide harboring Mdh2 N-terminus) or bidentate (Mdh2^{dimer}) inhibitor.
D. *In vitro* assay of Mdh2-6xHis testing effect of mutating several of its lysines (previously determined to be preferred targets of GID^{SR4} by mass-spectrometry) on Chelator-GID^{SR4}-dependent ubiquitylation. Mdh2-6xHis and its ubiquitylated versions were visualized by anti-6xHis immunoblotting.
E. Ubiquitylation model of Fbp1 (PDB: 7NS3, 7NS4, 7NS5, 7NSB; EMD-12557) involving juxtaposition of its target lysines (red and violet sticks, indicated by black circles) with Ubc8~Ub active sites (red stars) generated by: (1) docking of two Fbp1 degrons (black dashes) into substrate binding cavities of two opposing yGid4 molecules (red cartoon) and (2) rotation of the folded Fbp1 domain (brown cartoon) so that its target lysines could simultaneously reach both active sites (the recruited and activated Ubc8~Ub intermediate shown as cyan (Ubc8) and yellow (Ub) surface) modeled by aligning a previous RING-E2~Ub structure (PDB: 5H7S) with Gid2 RING (grey cartoon).
F. Ubiquitylation model of Mdh2 (blue cartoon; obtained by homology modeling) generated as in (B) but requiring a more pronounced shift of substrate receptor-scaffolding modules (Gid1-Gid8-Gid5-Gid4; grey cartoon) towards the center of the oval chelator assembly to enable capture of two Mdh2 degrons (black dashes). Unlike Fbp1, Mdh2 cannot be oriented so that its major target lysines (K330) from two protomers simultaneously engage both Ubc8~Ub active sites (red stars).

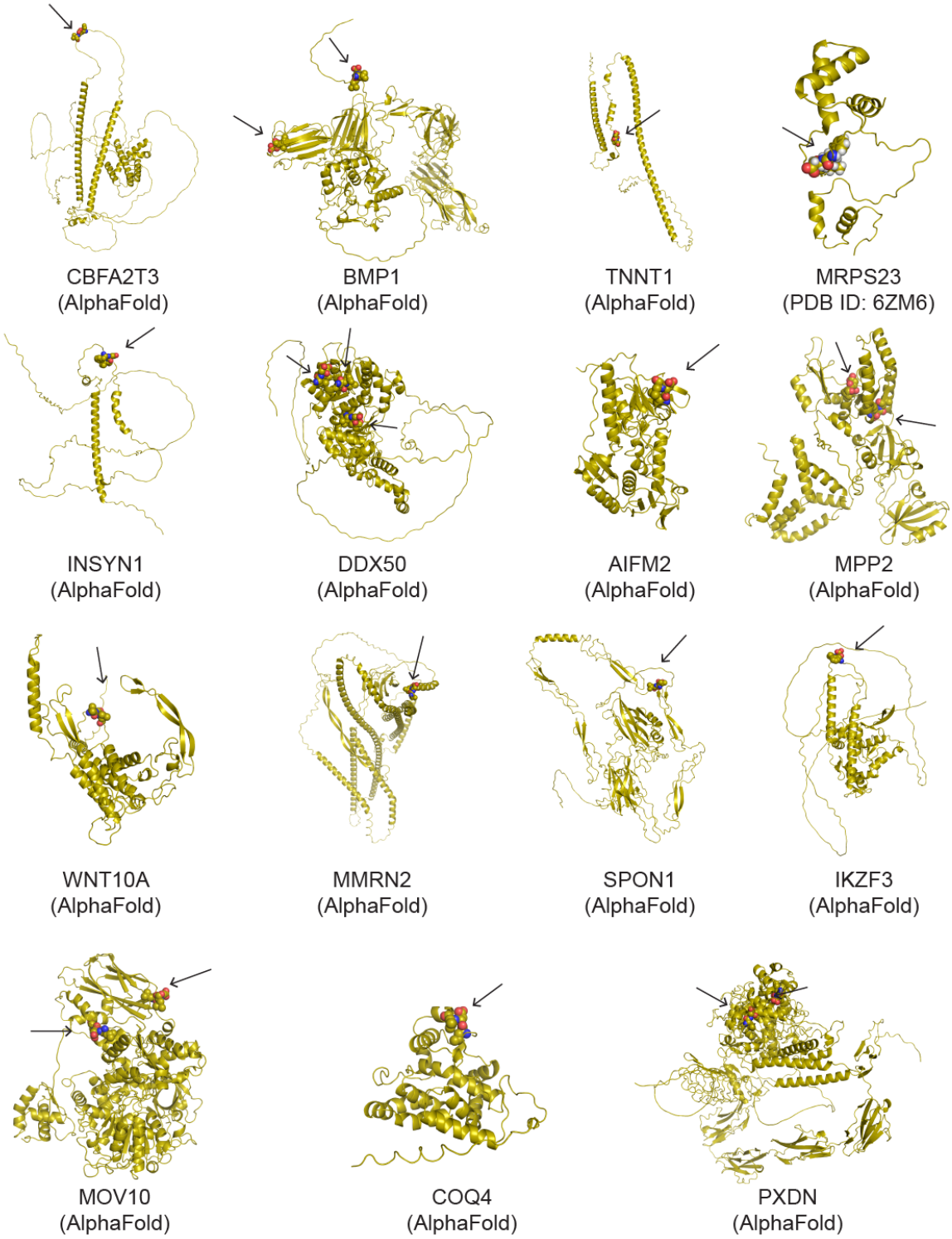

Figure S6: Structural analysis of proteins bearing the high-affinity hGid4-binding motif

BioGRID-annotated hGid4 interactors containing the solvent-exposed hGid4-binding [FIL]-D-[VIL] motif (indicated with black arrows). Solvent accessibility was assessed based on the PDB structures or AlphaFold models of the examined proteins.

	yGid10 + FWLPANLW	hGid4 + FDVSWFMG	hGid4 (without a peptide)
Data Collection			
Spacegroup	$P3_1$ 2 1	$P4_1$ 3 2	$P6_5$
Cell dimensions			
a, b, c (Å)	99.23 99.23 81.02	131.31 131.31 131.31	72.02 72.02 146.32
α, β, γ (°)	90 90 120	90 90 90	90 90 120
Resolution range (Å)	42.97 - 2.22 (2.30 - 2.22)	46.42 - 3.16 (3.27 - 3.16)	73.16 - 3.08 (3.19 - 3.08)
$I / \sigma (I)$	22.54 (1.29)	9.1 (1.0)	8.8 (1.0)
Completeness (%)	97.6 (85.1)	99.9 (99.6)	99.1 (96.2)
Refinement			
Refinement program	Phenix version 1.19	Phenix version 1.19	Phenix version 1.19
Resolution (Å)	2.22	3.16	3.08
R_{work} / R_{free}	0.19/0.22	0.24/0.29	0.24/0.27
Reflections used in refinement	22544 (2212)	7072 (690)	7950 (753)
Reflections used for R-free	1127 (88)	383 (39)	397 (38)
No. of molecules in ASU	1	1	2
Total no. of atoms	1848	1403	2737
Protein	1685	1332	2710
Peptide	75	62	0
Ligand	1	0	0
Water	87	9	27
Wilson B-factor ($Å^2$)	59.5	102.1	91.8
RMSD bond length (Å)	0.004	0.005	0.002
RMDS bond angle (°)	0.795	0.780	0.490
Ramachandran favored (%)	94.2	92.5	92.8
Ramachandran allowed (%)	5.8	7.5	7.2
Ramachandran outliers (%)	0	0	0

Table S1. X-ray crystallography data collection and refinement statistics

Values for the highest-resolution shell are given in parentheses.

sequence	GST-hGid4	GST-yGid4	GST-yGid10	GST
LDVSWFEM	2.722	2.499	0.22	0.135
WDVSWVSS	2.636	0.218	0.24	0.188
FDITGFIG	2.626	2.429	0.225	0.139
FDVGWFMS	2.614	2.506	0.275	0.368
FDVVRGIS	2.603	0.179	0.203	0.139
WDVSWASY	2.597	0.177	0.228	0.127
FDITGFLE	2.591	2.393	0.192	0.141
FDPSIMWG	2.579	2.064	0.23	0.146
FDITVFSG	2.574	2.353	0.158	0.162
VDVNSLWA	2.565	1.133	0.186	0.141
FDVARWWA	2.562	0.38	0.198	0.308
ITLSRVVT	2.554	0.172	0.229	0.132
FDVSGGMT	2.543	0.149	0.218	0.126
FDVSFWVR	2.542	0.636	0.186	0.159
IDIYSFLT	2.536	0.31	0.19	0.19
FDVYWFES	2.53	1.047	0.203	0.128
FDILWFDA	2.525	1.51	0.195	0.183
FIWIEPMS	2.51	0.165	0.192	0.158
FDLNWLQA	2.507	0.327	0.173	0.186
FDGASLRF	2.505	0.175	0.229	0.127
MDLSRLYL	2.504	0.166	0.184	0.147

sequence	GST-hGid4	GST-yGid4	GST-yGid10	GST
VDLTYFME	2.499	0.181	0.247	0.116
IGVLMNDM	2.491	0.148	0.173	0.192
FVWVWSVG	2.488	0.195	0.246	0.26
FIWLGESG	2.483	0.193	0.199	0.167
FDIGRGMT	2.48	0.174	0.184	0.139
IERVGYDL	2.446	0.178	0.21	0.145
FDAGRLFD	2.437	0.16	0.175	0.149
FDVSGVMS	2.432	0.144	0.159	0.138
FDVNFLQF	2.428	1.02	0.166	0.136
FDITGFSG	2.416	2.098	0.257	0.114
YDLGWFDN	2.406	0.148	0.158	0.139
IGLLPTEG	2.37	0.167	0.226	0.133
ISSSSSLV	2.332	0.207	0.234	0.151
FDVSRLSW	2.316	1.075	0.319	0.158
FDGSAFFW	2.258	0.132	0.171	0.135
MDAGVQYI	2.249	0.148	0.173	0.151
LDIFWATG	2.235	0.156	0.167	0.151
LGLLSAWA	1.992	0.176	0.173	0.162
LDVVLNRG	1.844	0.154	0.173	0.13
WVWDGGGH	1.493	0.183	0.18	0.149

Table S2. List of phage display-identified sequences binding hGid4 (Δ1-99) and yGid4 (Δ1-115)

Sequences were sorted and colored based on increasing intensity of phage ELISA signal for GST-hGid4 (Δ1-99) (from yellow to green; tested also for binding to GST-yGid4 (Δ1-115), GST-yGid10 (Δ1-56) and GST-only controls).

sequence	GST-hGid4	GST-yGid4	GST-yGid10	GST
FWLPANLS	0.313	0.197	2.074	0.261
AWLPPNIM	0.16	0.157	2.023	0.169
GFLPPNLV	0.208	0.189	1.911	0.146
GWLPQNLM	0.203	0.183	1.819	0.158
GFLPPNLL	0.13	0.128	1.729	0.119
GFLPPNLG	0.173	0.178	1.723	0.174
AWLPPNLE	0.194	0.167	1.691	0.141
AWLPPNVV	0.178	0.167	1.623	0.179
GWLPPNFR	0.203	0.178	1.263	0.147
FWLPPNQL	0.197	0.175	1.259	0.155
VWLPPNFY	0.214	0.183	0.655	0.165
ALLPENLR	0.151	0.15	0.644	0.151

Table S3. List of phage display-identified sequences binding yGid10 (Δ1-56)

Sequences were sorted and colored based on the intensity of phage ELISA signal for GST-yGid10 (Δ1-56) (from yellow to green; tested also for binding to GST-hGid4 (Δ1-99), GST-yGid4 (Δ1-115) and GST-only controls).